Hindawi
Advances in Meteorology
Volume 2019, Article ID 6792161, 13 pages
https://doi.org/10.1155/2019/6792161

Research Article

Influence of Regional Transport Mechanisms on the Fingerprint of Biomass-Burning Aerosols in Buenos Aires

Ana G. Ulke [1,2]

[1]*Departamento de Ciencias de la Atmósfera y los Océanos, Facultad de Ciencias Exactas y Naturales, Universidad de Buenos Aires, Buenos Aires C1428 EGA, Argentina*
[2]*UMI-IFAECI-CNRS-3351, Buenos Aires, Argentina*

Correspondence should be addressed to Ana G. Ulke; ulke@at.fcen.uba.ar

Received 25 January 2019; Revised 23 June 2019; Accepted 22 November 2019; Published 29 December 2019

Academic Editor: Harry D. Kambezidis

The study focuses on the transport of aerosol particles resulting from biomass burning in central South America towards the megacity of Buenos Aires by the South American Low-Level Jet. In particular, the cases are studied in which the exit area of the Jet reaches the La Plata Basin with no precipitation associated, herein called Chaco Jet 1 (CJ1), which could remove aerosols from the atmosphere on their way towards the city. CJ1 events registered within the five-year period of 2001–2005 are examined along with changes in the optical properties of aerosols over the city from measurements from the Aerosol Robotic Network (AERONET) site. Three-dimensional backward trajectories of CJ1 were obtained to verify the connection between the receptor site and the biomass-burning source region. A cluster analysis of the trajectories allows further characterizing the features and impacts of regionally transported aerosols. A subsample of days on which impacts of the contribution of biomass burning could have occurred, showed a statistically significant increase in aerosol optical depth and Ångström exponent, reflected by an increase in the peak of the derived volume size distribution in the fine fraction size range, which also shifts slightly towards bigger radii. The days with AOD greater than 0.15 show overall behaviour like other urban sites with pollution of different origins. The evaluation of the selected data reveals that higher values of AOD and changes in the Ångström exponent are linked to the dispersion of biomass-burning aerosols. Air mass trajectories coinciding with the CJ1 core present the strongest impact on aerosol characteristics, which can be seen in spectral measurements.

1. Introduction

The city of Buenos Aires is located on the southern shore of the Río de la Plata river. The city together with the 24 counties of the Greater Buenos Aires (GBA) is the third largest metropolitan area in South America with a population of nearly 13 million inhabitants [1]. Like every urban conglomerate, Buenos Aires is a source of anthropogenic pollutants and a receptor of contaminants from remote natural and anthropogenic sources. A common agricultural practice in rural areas of many countries around the world consists in burning native vegetation or agricultural residues for land clearing and preparation. During the dry season, also known as biomass-burning season, this practice gives rise to numerous fires. From July to December, the number of fires increases in northern Argentina, Bolivia, Paraguay, and south-central Brazil, with a peak from August to September [2–4]. Biomass burning introduces a variety of gases and particles into the atmosphere, such as black carbon, which results from incomplete combustion. Black carbon has a local warming effect on the atmosphere, affects cloud formation, and modifies the albedo of snow. As black carbon particles are short-lived (days to weeks), their effects are seen mostly on the regional scale [5].

Many studies focusing on the hydrological cycle and mesoscale convective systems demonstrated the relevant role of the South American Low-Level Jet (SALLJ) as a transport mechanism from tropical to mid-latitudes [6, 7]. Climatological studies of SALLJ events show that this northerly flow peaks at 17.5°S (Santa Cruz de la Sierra,

Bolivia) between 850 and 900 hPa and at a relatively lower altitude (900 hPa) at 23°S [7]. Observations made during the South American Low-Level Jet experiment (SALLJEX) revealed that maximum wind speeds varied in altitude from as low as 500 m to as high as 3 km within the domain; with higher altitudes during daytime hours [6]. SALLJ events have been classified according to the location of maximum flow. In this regard, most of the published research defines four SALLJ classes, one of which includes episodes exhibiting marked southward penetration, i.e., the Chaco Jet (CJ). Given its strong linkages with the development of mesoscale convective systems in northeastern Argentina during the warm season, research on the CJ is still going on [8].

The SALLJ also has an important role as a dispersion agent for biogeological material, as noted for the first time ever by Paegle [9] and later on by other authors [10–12] who studied aerosol transport drivers in southern South America. A subset of the Chaco Jet includes events that have no associated precipitation and a jet exit area in the La Plata Basin. That subset is known in the literature as CJ1 and is responsible for the regional transport of biomass-burning products from sources in central South America towards Buenos Aires. According to Castañeda and Ulke [13], CJ1 events, the most common SALLJ class, have the highest frequencies of occurrence in winter and spring, 16% and 10%, respectively, when all the days are considered. During August, the first month of the biomass-burning season, CJ1 occurrence increases sharply to 57% of the 16% occurrence in winter coinciding with the marked increase in the number of fire spots as seen in satellite imagery (see Figure 1, available at https://worldview.earthdata.nasa.gov).

Aerosol optical depth (AOD) is a measure of the extinction of solar radiation by aerosols and indicates the columnar aerosol load in the local atmosphere. The Ångström exponent represents the variation of AOD with wavelength. Larger Ångström exponents are typical for fine particles, while smaller values indicate the presence of coarse mode aerosols. Fine aerosol particles are typically urban/anthropogenic pollutants (combustion products from fossil fuel or biomass burning) whereas those associated with natural sources belong to the coarse fraction (dust, marine aerosol, volcanic ash, and bioaerosol). The variables described are measured continuously at numerous sites worldwide by the AERONET network. One of such sites, CEILAP-BA, is located in Buenos Aires, at 34.57°S, 58.50°W, 26 m a.s.l. CEILAP-BA is operational since 2000 and is located near the boundary between the city and the northern region of GBA and close to a highly busy highway.

A preliminary study reported noticeable increases in mean AOD and Ångström exponent during CJ1 events during the biomass-burning season using AERONET V2.0 data [14]. Studies of the role of the SALLJ in the regional transport of biomass-burning products in 2002 using observational data and modelling tools provided a detailed three-dimensional structure and evolution of the meteorological and aerosol fields [10, 15].

Concerning the typical values of the Ångström exponent for biomass-burning aerosols, important annual variability in Alta Floresta, Brazil, with maxima higher than 1.5 from July to October was reported [16, 17]. These results are consistent with findings in the analysis of smoke particles, with values ranging from 2.5 for fresh smoke to 0.5 for aged smoke [18]. Physical, optical, and chemical characteristics of aerosols transported by the CJ1 and reaching Buenos Aires might undergo transformations along their trajectories. According to Reid et al. [18], aerosol particles undergo an ageing process over a period ranging from one to four days during which they increase in average size. Coagulation and condensation processes were found to account for the growth of particles in the fine mode, reaching characteristic radii of about 0.2 μm [19].

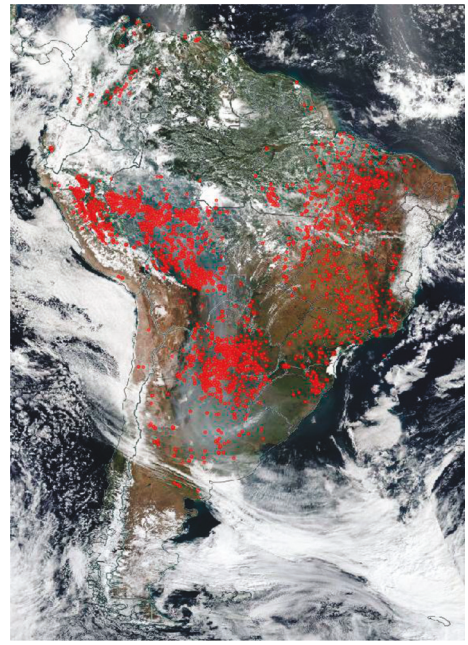

Figure 1: Smoke plume and fire spots on 26 August 2016 (available at https://worldview.earthdata.nasa.gov).

Ångström exponent differences correspond to a curvature in the spectral dependence of optical depth. As shown by Kaufman [20], negative Ångström exponent differences reveal the dominance of fine mode aerosols, whereas positive values are indicative of the effect of two distinct modes. Increases in optical depth associated with increases in Ångström exponent and decreases in Ångström exponent difference are due to the growth of the concentration of the accumulation mode relative to the coarse particle mode.

Eck et al. [21] showed that biomass burning and urban aerosols exhibit large spectral variations of the Ångström exponent at moderate to large optical depths due to the dominance of fine mode sized particles. They suggest that information on curvature be utilized in conjunction with Ångström exponent to characterize more fully the dependence of AOD on wavelength. Aerosol size distributions with significant coarse mode (such as desert dust) present very little spectral variation of the Ångström exponent and the value of the Ångström exponent itself provides useful information on the relative influence of coarse versus fine mode aerosols. This relative influence between modes also applies for low optical depth urban and biomass-burning aerosols.

Several methods have been developed to determine the occurrence and apportionment of fine and coarse modes, as well as the variation of the Ångström exponent [22, 23]. A graphical framework to visualise the relationships between the Ångström exponent and Ångström exponent difference, along with the contribution of fine aerosols to the AOD and the size of the fine particles was proposed by Gobbi et al. [24]. The method allows classifying aerosol properties, and it is appropriate for identifying aerosol modification processes (i.e., hydration, coagulation, and cloud contamination). Gobbi et al. [24] presented the analysis for three groups of selected AERONET sites: Beijing (China), Rome (Italy), and Kanpur (India), characterized by urban pollution and contributions of mineral dust; Ispra (Italy), Mexico DF (Mexico), and GSFC (USA), typical urban pollution; and finally Mongu (Zambia) and Alta Floresta (Brazil), which are strongly influenced by biomass-burning pollution.

The results reported in the present paper are intended to contribute to the understanding of aerosol optical properties in the atmosphere of Buenos Aires and to document the impact on those properties of regional flow during aerosol transport from remote sources.

The paper is structured as follows: Section 2 describes the data and methodologies applied; Section 3 examines aerosol optical properties and the influence of the CJ1 low-level jet type; and Section 4 presents the main findings and conclusions.

2. Methodology

The occurrence of CJ1 events was diagnosed applying the modified Bonner criteria on GDAS (Global Data Assimilation System) data provided by NCEP (National Centers for Environmental Prediction) for the period 2001–2005 as detailed in [13].

The AErosol RObotic NETwork (AERONET, http://aeronet.gsfc.nasa.gov) provides a freely available, unique, continuous, and high-quality database for the study of aerosol features and behaviour. Detailed information on the retrieval, inversion algorithms, and quality-control procedures can be found in [21, 22, 25–28] or on the AERONET web page. Version 3 AOD data, which have been released recently [29], are available at three data quality levels: Level 1.0 (unscreened), Level 1.5 (cloud-screened and quality controlled), and Level 2.0 (quality-assured). AERONET data, from the CEILAP-BA site, used in this study were V3.0 level 2 data of (a) columnar aerosol load at 500 nm (AOD500nm), (b) Ångström exponents derived from wavelengths of 440–870 nm (AE_440-870nm), 440–675 nm (AE_440-675nm), and 675–870 nm (AE_675-870nm), and (c) aerosol volume size distributions.

Basic statistical parameters of AOD500nm and AE_440-870nm for the period 2000–2016 were calculated to determine their climatological values. In addition, the same parameters were calculated using the daily data available in the five-year period from 2001 to 2005. Statistical significance tests (t-test) of changes in the mean values of aerosol properties between those days with and without the influence of biomass burning were applied, and the results are summarized in Table 1. This approach considers changes in optical and physical properties by merging them into mean values; such smoothing contributes to enhance the results of the comparison. The significance of the null hypothesis: "aerosol properties (AOD500nm, AE_440-870nm, and volume size distributions) on biomass-burning days are statistically the same as on no-burning days" was tested. For each case, the significance was checked by means of the p value ($p < 0.05$ for statistically significant variations at the 95% confidence level).

Three-dimensional backward trajectories reaching CEILAP-BA were obtained with the HYSPLIT 4.9 model (HYbrid Single-Particle Lagrangian Integrated Trajectory) of the Air Resources Laboratory (ARL), National Oceanic and Atmospheric Administration (NOAA) [30, 31]. The model was run using meteorological data from the Final Run analysis for the Southern Hemisphere (FNL-SH) provided by ARL/NOAA. Backward trajectories were calculated for the main standard synoptic times, 00, 06, 12, and 18 UTC, for the five-year period. Four levels were considered: 35, 500, 1000, and 1500 m a.s.l. Transit time of the air masses reaching Buenos Aires was set at 72 hours, in accordance with the regional transport time by CJ1 and the typical variability of the synoptic environment at the latitude of interest. Vertical velocity was calculated assuming isentropic processes to allow following air masses and detecting frontal surfaces.

The selection of situations associated with the regional transport of biomass-burning products to Buenos Aires was based on a four-step procedure. Firstly, CJ1 events were identified. Flow in this category extends latitudinally to Buenos Aires or even farther south. This requirement ensures the rapid displacement of air parcels towards the region of interest. Secondly, for the corresponding date, daily AOD500nm from the AERONET database was required to be greater than the climatological monthly mean. Thirdly, at least one of the four trajectories was required to have originated at or travelled over the area, herein considered as the "biomass-burning source region," which includes north-eastern Argentina, Paraguay, Bolivia, and the Brazilian states of Goias, Mato Grosso, Mato Grosso do Sul, and Rondônia. The fourth and final step consisted of verifying whether biomass was being burnt along the path of the air parcels. To this end, satellite imagery provided by the Instituto Nacional de Pesquisas Espaciais (INPE, National Institute for Space Research), Brazil (http://www.inpe.br/queimadas/bdqueimadas) was analysed to determine the number and location of fire spots.

The temporal evolution and relationship between aerosol optical properties and derived size characteristics were analysed for associated biomass-burning signatures. The classification diagram proposed by Gobbi et al. [24] was used to analyse aerosol spectral observations. The method consists of a visualization scheme based on the analysis of AE_440-870nm, the spectral curvature (represented by the difference between AE_440-675nm and AE_675-870nm), AOD in terms of fractional contribution of fine particles to total AOD (η = AOD fine/AOD total), and the size of fine mode material (R_f). The scheme is based on Mie scattering for a complex refractive index typical for urban/industrial aerosols. Gobbi et al. [24] assume a bimodal aerosol size distribution, and their analysis of the sensitivity to the refractive index

Table 1: Basic statistical parameters for AOD500nm and AE_440-870nm based on daily data.

Group 1 all data 2001–2005	All (*a*)	BB (*b*)	No BB (*c*)	*a* & *b* *t* *p*	*a* & *c* *t* *p*	*b* & *c* *t* *p*
AOD mean	0.128	0.168	0.109	**3.70** **<0.001**	**2.83** **0.005**	**5.86** **<0.001**
AOD sd	0.144	0.209	0.095			
AE mean	1.243	1.287	1.223	*1.68* 0.09	*1.01* 0.31	***2.33*** **0.02**
AE sd	0.385	0.382	0.385			
N	915	288	627			
Group 2 selected days (+)	All (*a*)	BB (*b*)	No BB (*c*)	*a* & *b* *t* *p*	*a* & *c* *t* *p*	*b* & *c* *t* *p*
AOD mean	0.360	0.549	0.182	**2.98** **0.004**	**3.57** **< 0.001**	**6.69** **< 0.001**
AOD sd	0.288	0.312	0.071			
AE mean	1.566	1.638	1.498	1.57 0.12	1.44 0.15	**2.68** **0.009**
AE sd	0.222	0.195	0.227			
n	68	33	35			
				1a & 2a *t* *p*	1c & 2c *t* *p*	1a & 2c *t* *p*
AOD				**11.69** **<0.001**	**9.34** **<0.001**	**4.43** **<0.001**
AE				**6.82** **<0.001**	**5.18** **<0.001**	**4.18** **<0.001**

For each group and parameter, the first column presents the results for the whole data set (all) and the second and third columns correspond to the biomass-burning season (BB) and no-burning period (no BB) for each subgroup. The *t* and *p* values are the statistical variables of the *t*-test. Statistically significant differences (95% confidence level) between groups are highlighted in bold.

indicates that the maximum R_f indetermination is about ±25% while η spans a range in the order of ±10%. Particle nonsphericity is assumed not to affect the results significantly [24]. Within this level of indetermination, the scheme is considered robust enough to provide an operational classification of aerosol properties and their modification processes in the atmosphere (humidification and/or coagulation, cloud contamination or inclusion of coarse mode particles).

The visual criteria described above are used to characterise aerosol features and possible modification processes. The dominance of fine-mode aerosols is related to negative dAE (dAE = AE_440-675nm − AE_675-870nm) associated with larger AE (AE_440-870nm). Positive or near zero dAE values indicate the presence of two separate modes with larger contribution of coarse-mode particles. Aerosols that underwent modification processes (ageing, coagulation, humidification, and cloud contamination) have distinct characteristics in the AE vs. dAE scheme. The increase in AOD with R_f and η suggests the humidification of aerosols, while an increase in AOD with increasing R_f and decreasing AE indicates ageing and/or coagulation. The reverse, increase in AOD with decreasing R_f and increasing AE, corresponds to freshly emitted fine aerosols [24, 32, 33]. The rise in AOD with coarse-mode fraction along a constant R_f curve towards the origin AE = dAE = 0 points to cloud contamination. Similarly, the increase in AOD towards lower AE and smaller negative dAE values indicates the presence of either dust or maritime aerosols or a combination of both.

Transport patterns and associated atmospheric conditions were characterized by means of cluster analysis of trajectories reaching Buenos Aires. In the clustering process, trajectories are combined until the total variance of individual trajectories with respect to the cluster mean starts to increase. The spatial variance relates the endpoints of the cluster's component trajectories and the mean of the trajectories in that cluster. The spatial variance of a cluster is the sum of the spatial variance of all trajectories within that cluster. The total spatial variance is the sum of the cluster spatial variance over all clusters [34].

Composites of the corresponding synoptic fields were calculated using GDAS analysis to show the main features of the meteorological conditions associated to each trajectory cluster.

3. Results and Discussion

Figure 2 illustrates the monthly means and standard deviations of AOD and the Ångström exponent. Mean AOD and its standard deviation are greater during the biomass-burning season, which extends from August to October, with slightly higher values in August. Monthly AOD mean and standard deviation are in the same order of magnitude. The standard deviation of the Ångström exponent is small compared with the monthly mean, which indicates low variability of this variable. Yearly climatological values for Buenos Aires are: AOD500nm = 0.114 ± 0.1 and AE_440-870nm = 1.15 ± 0.4, respectively.

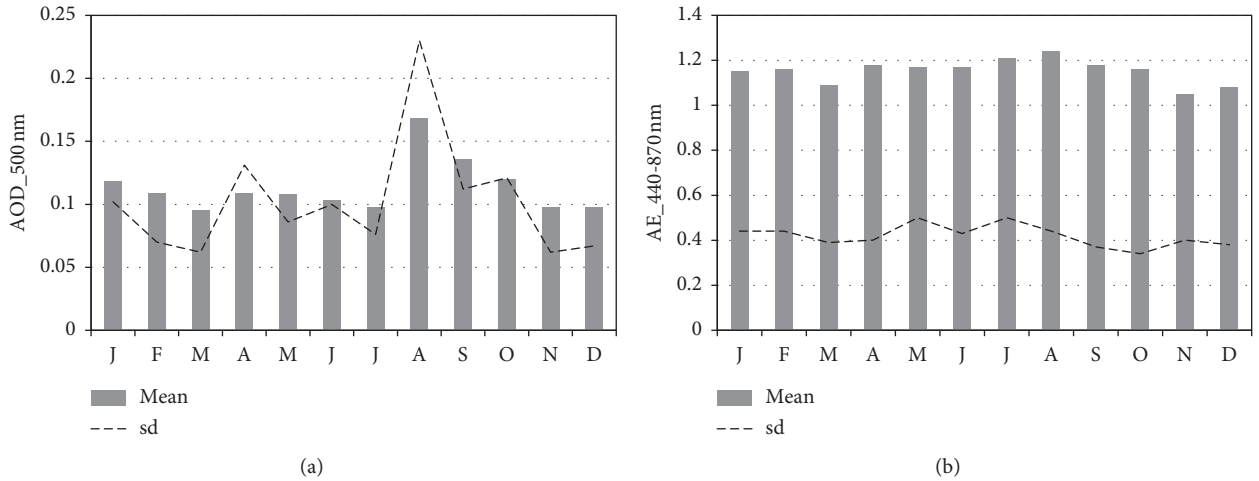

Figure 2: Monthly means and standard deviations of AOD500nm (a) and Ångström exponent (b) at CEILAP-BA (climatological values for the period 2000–2016).

The selection of events meeting the set of criteria, i.e., with possible regional transport of biomass-burning products towards Buenos Aires, made it possible to identify a total of 68 days within the five-year period under analysis. In agreement with the synoptic environment associated to CJ1 events, on six occasions, the selection criteria were met on several consecutive days. The longest of such spells in the analysed period took place from 24 to 27 August 2002 and was first reported in a case study in 2006 [35].

The evolution of AOD and the Ångström exponent values is shown in Figure 3. The climatological means along with their standard deviations are also included. Figure 3(a) shows that on most days of the period under study, daily values of AOD are smaller than the climatological mean. This would indicate that in general, the aerosol load in BA is low. Exceedance cases above the climatological mean and above the average plus one standard deviation are of greater concern in terms of environmental impact. The cases included in the selected dates (denoted with +) belong to the latter groups. However, such exceedances are also found in the set of remaining days. In general, the remaining days have low, smaller than the average, AOD values (which represent 71% in the subset of remaining days, and 6% in the subset of selected days). AOD values above the average plus one standard deviation are observed in 7% of the remaining days and 51% of the selected days. The variability of daily AE values can be seen in Figure 3(b). Most of those values are greater than the climatological mean and even greater than the average plus one standard deviation (which represent 58% of the remaining days and 98% of the selected days). Values bigger than the average plus one standard deviation are 18.6% of the remaining days and 63% of the selected days. Although, in general, mean values are low compared with those of other cities and sites located in the area of biomass burning, the increase in AOD over Buenos Aires during the burning season would be caused by relatively remote sources, which would indicate the presence of regional transport.

Figure 4(a) depicts the relationship between daily AOD and the Ångström exponent on the biomass-burning days selected (black diamonds) and the remaining days (open circles). While the large dispersion of the whole data set reflects the varied nature of aerosols over Buenos Aires, the days selected show the typical features reported in the literature for biomass-burning aerosols [21, 36, 37]. For the latter, increased AOD values are associated with Ångström exponents ranging from 1 to 2.

To further explore the role of CJ1 as the transport mechanism, Figures 4(b) to 4(c) present the variation of AOD with Ångström exponent for the biomass-burning season (Figure 4(b)) and for the remaining months (Figure 4(c)). Although a distinctive pattern is not evident when comparing the biomass-burning season to no-burning months, the selected days point to a connection between CJ1 regional transport and the rise in AOD and Ångström exponent, as clearly shown in Figure 4(d). On the selected days and during the biomass-burning season, the Ångström exponent values are 1.24 to 2 for AODs ranging from 0.2 to 1.25.

Table 1 presents some basic statistic parameters of aerosol optical depth and Ångström exponent in the whole 2001–2005 period, as well as in biomass-burning (BB) and no-burning months (no BB) along with the comparison with the values for the selected days. The statistical analysis of the differences between the mean values of AOD and AE of the whole data set (group 1) and the selected cases (group 2) showed statistical significance at the 95% confidence level. This holds for the comparison between all the data (group 1a and group 2a) and the subsamples for BB (group 1b and group 2b) and no BB days (group 1c and group 2c) (see Table 1). These results are in agreement with the imposed conditions for the selection of days with regional transport of biomass-burning aerosols by the CJ1.

The significance of the differences between the mean values within each group was also tested. Statistically significant differences are observed in all the comparisons for AOD. In contrast, changes in the AE are significant only when the BB and no BB subsamples are considered.

The comparison of the mean volume size distributions for all the data over the period 2001–2005 with those of the

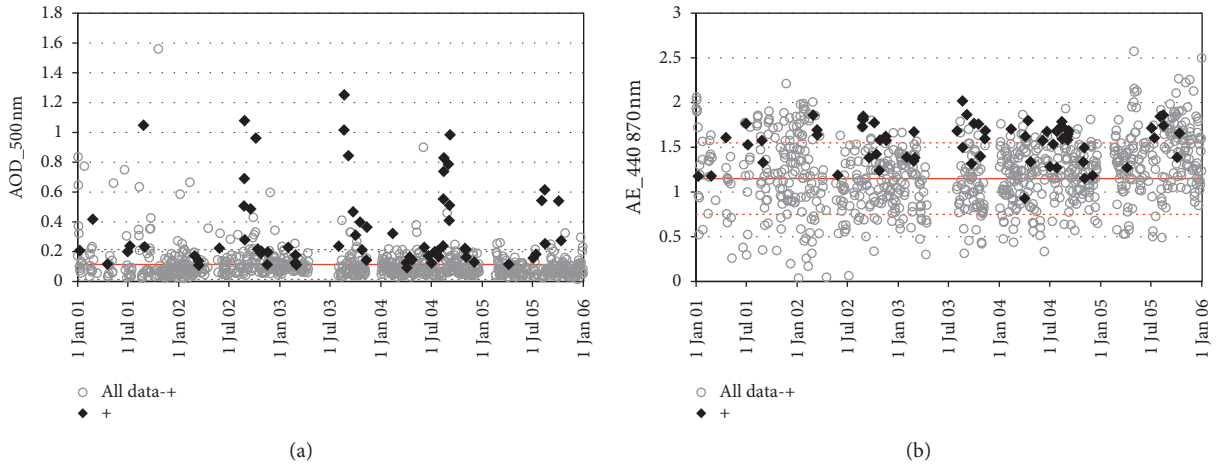

FIGURE 3: Temporal evolution of daily AOD500nm (a) and Ångström exponent (b) at CEILAP-BA in the five-year period 2001–2005. Black diamond: days with regional transport of biomass-burning aerosols (selected dates). Open circle: daily data with the selected days excluded. + denotes the "selected dates." The climatological means and standard deviations are included (red lines).

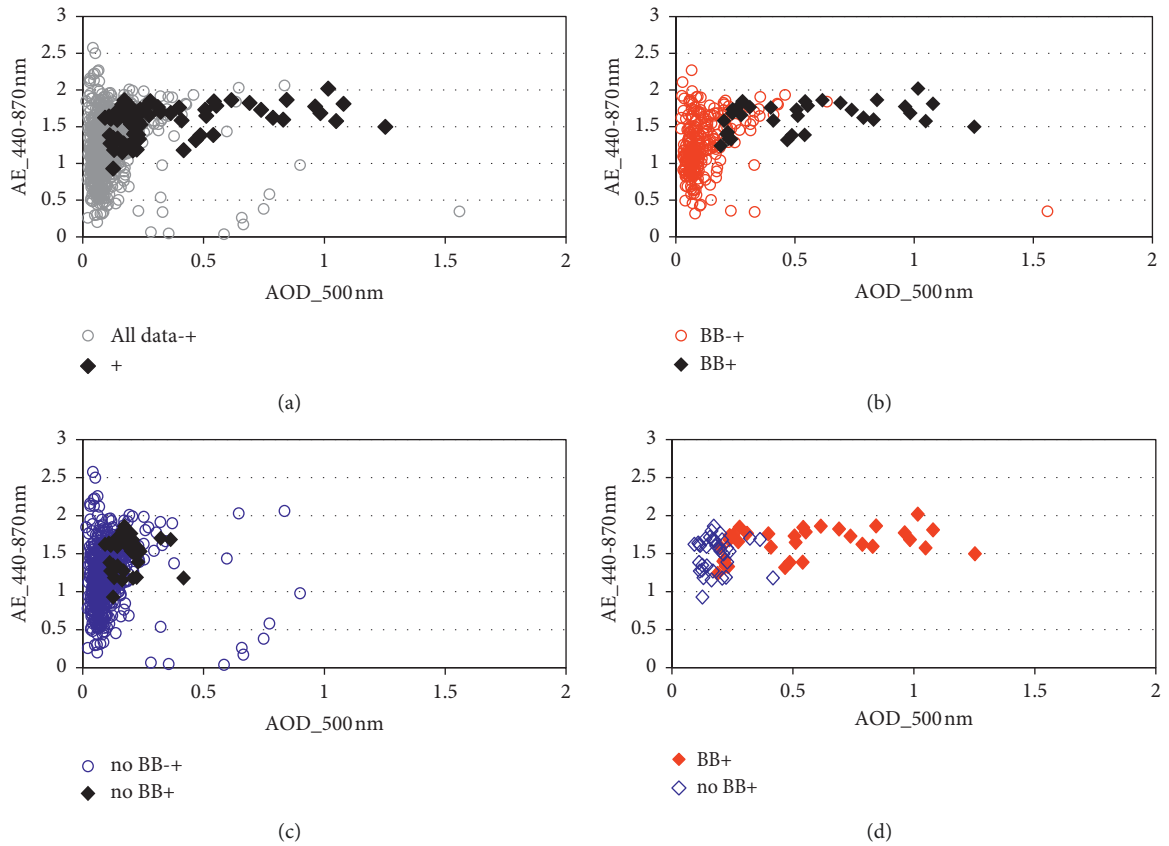

FIGURE 4: Variation of Ångström exponent with AOD500nm at CEILAP-BA in the five-year period 2001–2005. (a) Black diamond: days with regional transport of biomass-burning aerosols (selected dates). Open circle: daily data with the selected days excluded: (b) same as (a) during biomass-burning months (August to September); (c) same as (a) during no-burning months; and (d) days with regional transport of biomass-burning aerosols, red diamond: biomass-burning months, and blue diamond: no-burning months. + denotes the "selected dates."

selected days is presented in Figure 5(a). For the whole data set, concentrations of coarse and fine modes are almost similar, whereas for the group of selected days, a rise is observed in the concentrations, which is more pronounced in the fine mode. The comparison of biomass burning and no-burning periods shows that distributions are similar in the coarse mode whereas a slight increase in the fine mode is observed in the biomass-burning season (Figure 5(b)). A

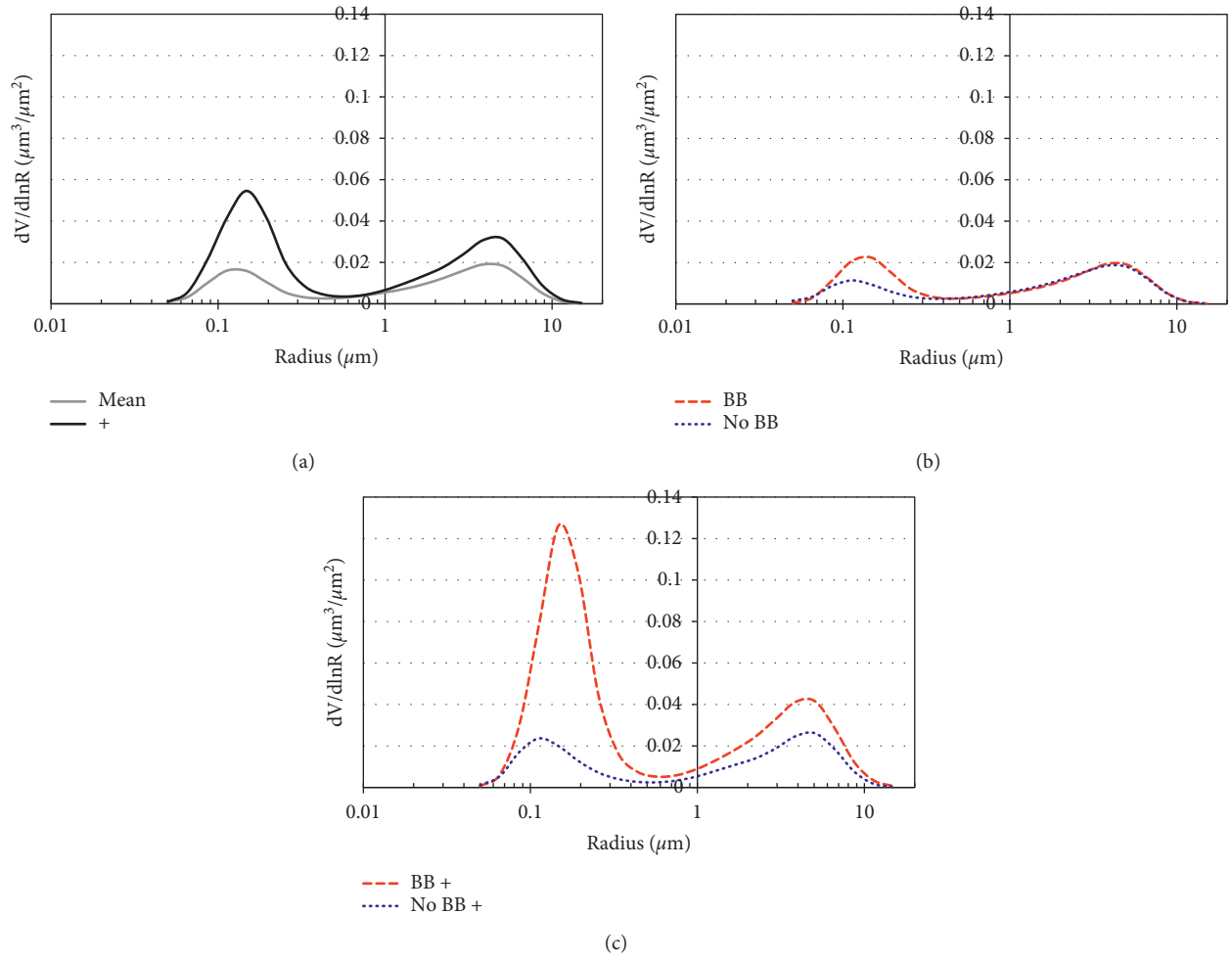

Figure 5: Mean volume size distributions of aerosols at CEILAP-BA. (a) Comparison of size distributions between the entire period and selected days, black line: days with regional transport of biomass-burning aerosols and grey line: all days; (b) comparison of size distributions for all days during the biomass-burning months (red line) and no-burning months (blue line); (c) comparison of size distributions for the selected dates during biomass-burning months (red line) and no-burning months (blue line). + denotes the "selected dates."

similar analysis of the size distributions for the selected days depicts the clear impact of CJ1 as a transport agent of biomass-burning aerosols (Figure 5(c)). These results are consistent with published research ([38, 39], among others).

The difference between the volume size distributions in the 2001–2005 period and the selected days (Figure 5(a)) is at the limit of statistical significance (p value~0.047). The differences in the volume size distributions between the whole data set in the BB period and the selected days in the BB period (Figures 5(b) and 5(c) red dashed line) are statistically significant (p value <0.05). The same holds for the comparison between the volume size distributions for the selected days in the BB (Figure 5(c) red dashed line) and those during the no BB months (Figure 5(c) blue dotted line).

In view of the above, the null hypothesis is rejected because AOD and AE in Buenos Aires have statistically significant increases on biomass-burning days. These significant differences are consistent with significant modifications in the mean volume size distributions, with a five-fold increase in concentration in the fine mode fraction together with a shift towards higher fine modal radii. A smaller impact is also observable in the coarse fraction. However, it is to be noted that aerosol size distributions from almucantar retrievals are fewer than the spectral measurements. Therefore, these relationships should be analysed cautiously.

At this point, it is worth highlighting that statistical differences on mean aerosol properties provide compelling evidence of the role of CJ1 in the transport of biomass-burning aerosols towards Buenos Aires. However, the analysis of the relationships between variables on a daily basis would help advance the understanding of the phenomenon.

Figures 6 and 7 show the classification scheme proposed by Gobbi et al. [24] including the daily data with AOD greater than 0.15, in order to keep errors below 30% in AE and dAE and to make comparisons possible of the results in this study with other results published in similar studies ([24, 32, 40–42], among others). Figure 6 includes the whole data set for the period 2001–2005 and Figure 7 shows the data on the selected days thus focusing on the changes in the

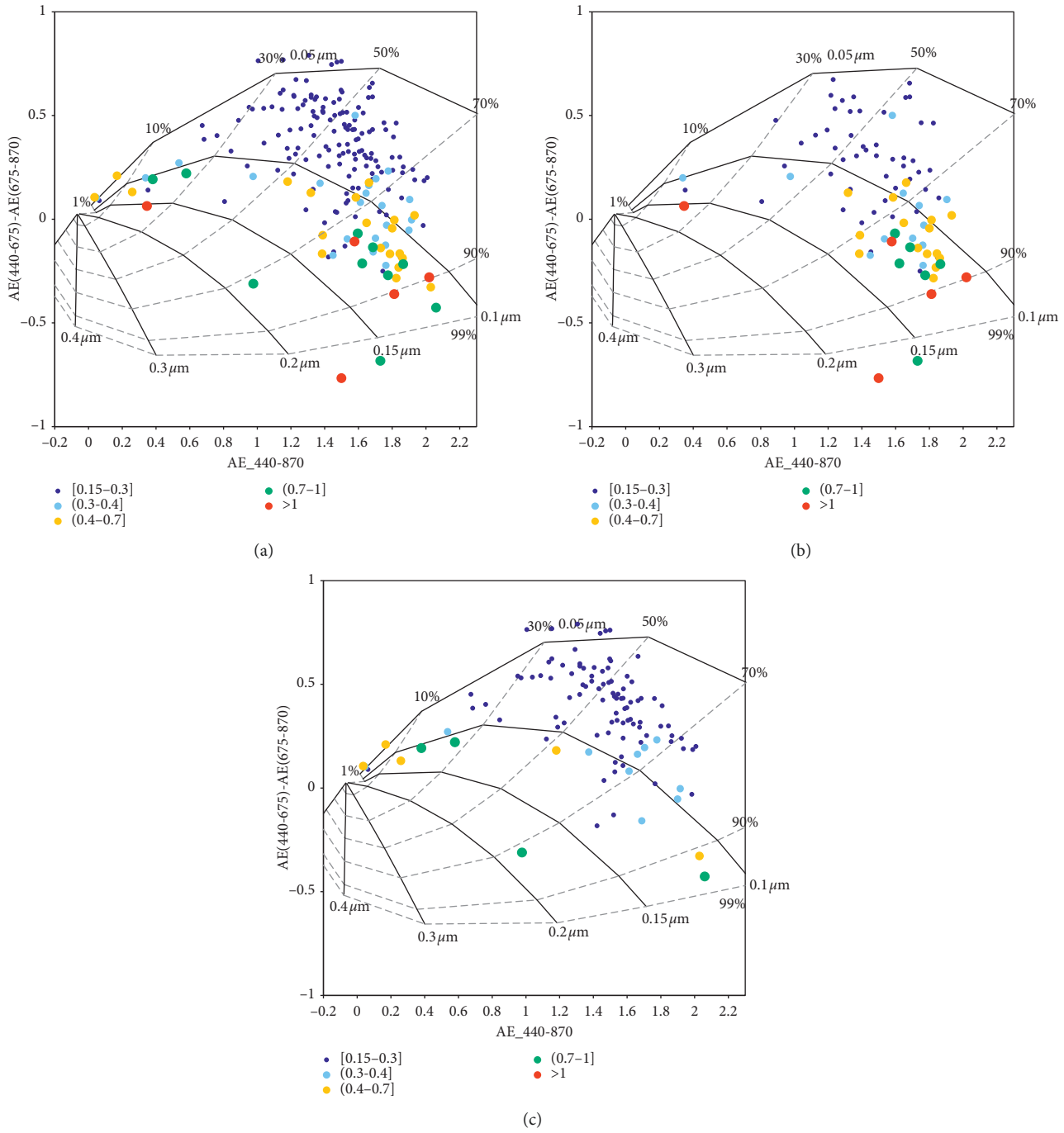

Figure 6: Ångström exponent difference as a function of the Ångström exponent and AOD (colour code) for CEILAP-BA. Only data with AOD500nm greater than 0.15 are included: (a) all days in the selected period (2001–2005); (b) all days during the biomass-burning months; and (c) all days in no-burning months.

AE vs. dAE pattern between the two groups. CEILAP-BA data indicate aerosols over Buenos Aires are mainly composed of anthropogenic pollution (urban/industrial and biomass-burning particles) along with sporadic presence of natural aerosols, dust, sea-salt, from arid or ocean areas located in the region.

The comparison with published studies [24, 32] suggests that aerosol features in the atmosphere over Buenos Aires are similar to those of urban areas, e.g., Ispra, Mexico, Rome, and GSFC, with the addition of some characteristics from places where the biomass-burning signature is dominant, such as Mongu and Alta Floresta.

For AOD in the smallest range (from 0.15 to 0.3), AEs greater than 1 are associated with positive dAE which indicates the presence of two aerosol modes and fine mode contributions to total AOD (η) ranging between 30 and 70%. The fine fraction is characterized by smaller R_f values ranging from 0.05 μm to 0.1 μm.

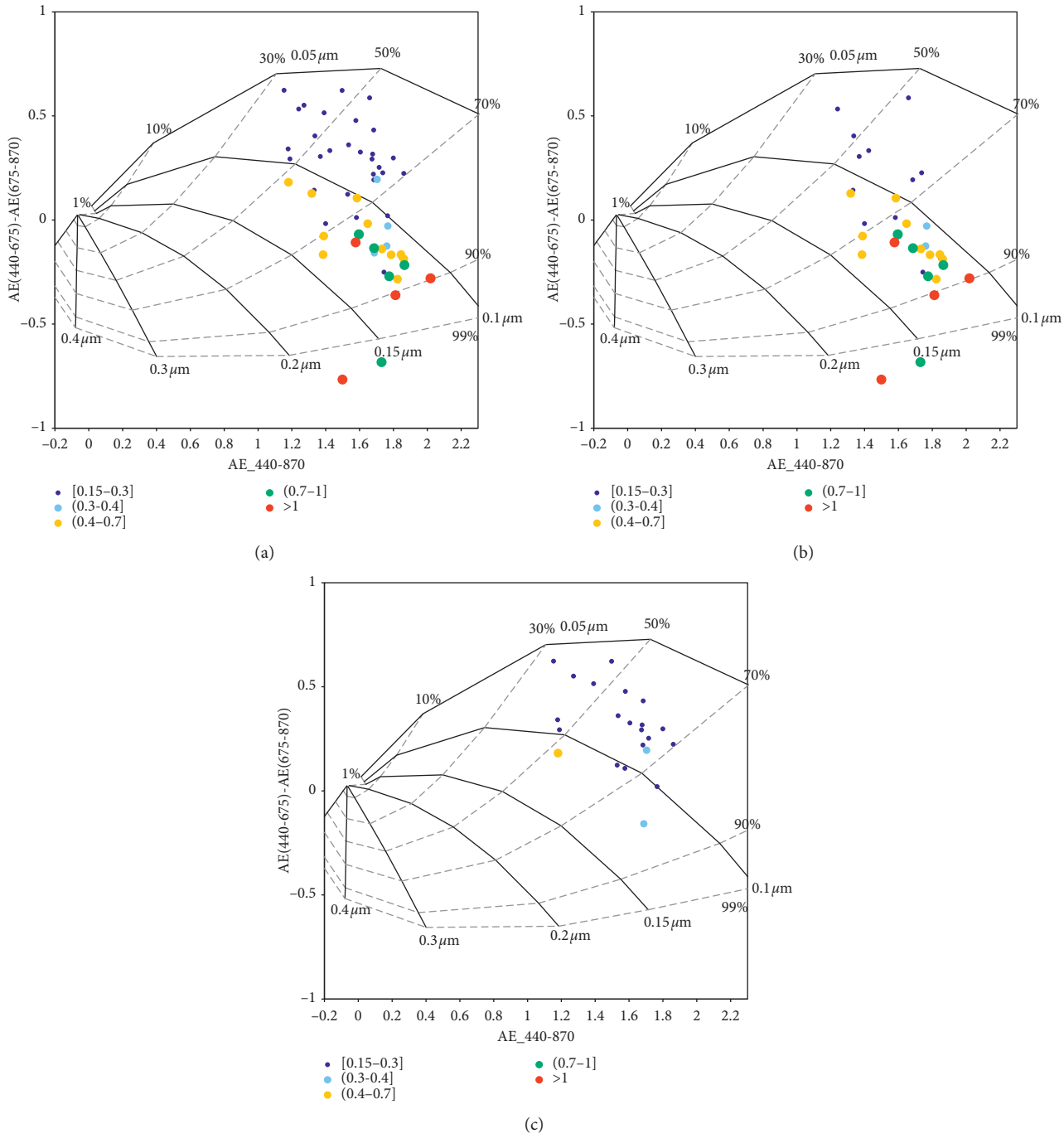

Figure 7: Ångström exponent difference as a function of the Ångström exponent and AOD (colour code) for CEILAP-BA. Only data with AOD500nm greater than 0.15 are included: (a) selected days; (b) selected days during biomass-burning months; and (c) selected days in the remaining months.

Higher AODs (from 0.3 to >1) are mainly associated to Ångström exponents greater than 1.4 and negative dAE, suggesting the dominance of fine-mode aerosols from anthropogenic origin. The fine mode fraction of AOD values ranges from 70 to 90% and R_f is between 0.1 μm and 0.15 μm. The fine particle sizes (R_f) show an increasing trend while their contribution to AOD (η) and total AOD grows, which suggests aerosols were undergoing an ageing process associated to hydration and/or coagulation under turbid conditions [24, 32, 33, 41, 43].

Few data points were identified with the dAE~0, low AE < 0.5, and η < 30%. Those aerosol characteristics would suggest a sporadic contribution of coarse-mode aerosols (dust or sea salt) associated with air masses travelling from arid regions or the adjacent oceans. This was also observed by [32, 40, 43–47]. Isolated cases of high turbidity and

increased R_f (between 0.15 μm and 0.2 μm) could be related to the occurrence of specific events that would deserve further investigation.

The splitting of the sample into biomass-burning and no-burning months (Figures 6(b) and 6(c)) illustrates the increase in aerosol load, Ångström exponent, and fine mode contribution along with more negative dAE during burning months with the changes in AOD mostly associated to the concentration of fine mode particles. The more negative dAE with increasing AOD is an indication of fine mode dominance as is also observed over biomass-burning regions [24, 33, 48, 49]. Contrarily, no-burning months present the smallest AODs, positive dAE values, and η ranging from 30% to 70%. The few data points associated to coarse particles near the origin occur in no-burning months.

A remarkable feature observed in the group of days selected because of the influence of biomass burning (Figure 7(a)) is the reduction in the number of days with the lowest atmospheric turbidity, i.e., smallest range of AOD (from 0.15 to 0.3). Most of the observations have spectral signatures in the negative range of Ångström exponent differences, larger AOD, Ångström values greater than 1.4 and fine fraction contribution to AOD greater than 70%. The resulting classification scheme for the selected cases during biomass-burning and no-burning seasons (Figures 7(b) and 7(c)) show the impact on aerosol load and features resulting from the regional transport of biomass-burning aerosols driven by CJ1.

The first condition for the selection of the cases of interest is the occurrence of a CJ1 type of SALLJ, thus imposing a common feature to the regional flow. However, the variability of the meteorological environment associated to this category might cause some differences in the transport patterns and aerosol properties. A trajectory cluster analysis was used to help find those influences. A final number of four clusters was set at the point where abrupt changes in total spatial variance were observed.

Figure 8 presents the mean trajectories of the air masses reaching Buenos Aires on the selected days in each cluster. Cluster 1 includes trajectories with the shortest travel distances, originating mainly over north-eastern Argentina, a few coming from Paraguay and Southern Brazil. Trajectories with origin in the southernmost states of Brazil that turn counter-clockwise (anticyclonic gyre in the Southern Hemisphere) to travel towards the easternmost provinces in Argentina belong to cluster 2. Cluster 3 includes trajectories originating or travelling over the Brazilian states of Goias, Mato Grosso, and Mato Grosso do Sul and turning counter-clockwise to flow over central Paraguay and north-eastern Argentina with N-S direction. Finally, cluster 4 is the one including the trajectories originating in Northern and Central Bolivia, travelling over western Paraguay and north-eastern Argentina with NW-SE direction.

Figure 9 shows the composite wind fields and the area where the CJ1 occurrence criteria are met in each cluster. In all the cases, flow direction is towards the city, passing over locations where biomass is being burnt. Fields are consistent with the mean trajectories in the clusters. The jet events included in clusters 3 and 4 are stronger and more extensive.

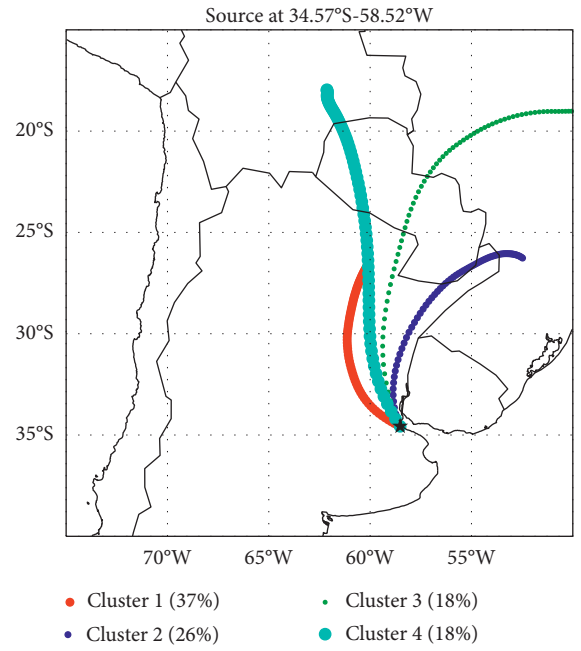

Figure 8: Cluster mean trajectories arriving at CEILAP-BA during the selected days. Trajectory widths indicate variability in the spatial path of each cluster. The percentage contribution of each cluster is also indicated between brackets.

Table 2 lists the mean spectral properties obtained from CEILAP-BA observations for each cluster. In all cases, values are greater than the climatological means. Cluster 4 is the one that shows the highest impact of biomass-burning products, i.e., it has the greatest mean AOD and Ångström exponent. This group is followed by cluster 3, with evidence of relative dominance of fine mode aerosols, but smaller total aerosol content. In all clusters, the analysis of the groups of biomass-burning and no-burning days shows that mean AOD and Ångström exponent values are significantly higher during the burning season. This confirms the role of CJ1 transport patterns in relating biomass-burning with the changes in aerosol features farther downwinding.

4. Conclusions

This paper studied the possible contributions to changes in aerosol load and properties in the atmospheric column over Buenos Aires, caused by the regional transport of biomass-burning products by the CJ1 type of the South American Low-Level Jet-SALLJ. Five-year spectral observations at the Buenos Aires AERONET site, CEILAP-BA, were analysed. Information provided by those observations was complemented with an evaluation of low-level meteorological patterns in southeastern South America and of the occurrence of biomass burning.

Selected spectral observations were aerosol optical depth at 500nm, the Ångström exponent at different wavelength pairs, and the derived particle volume size distributions. Averages and standard deviations of AOD and AE were obtained from the observations for the period 2001–2005

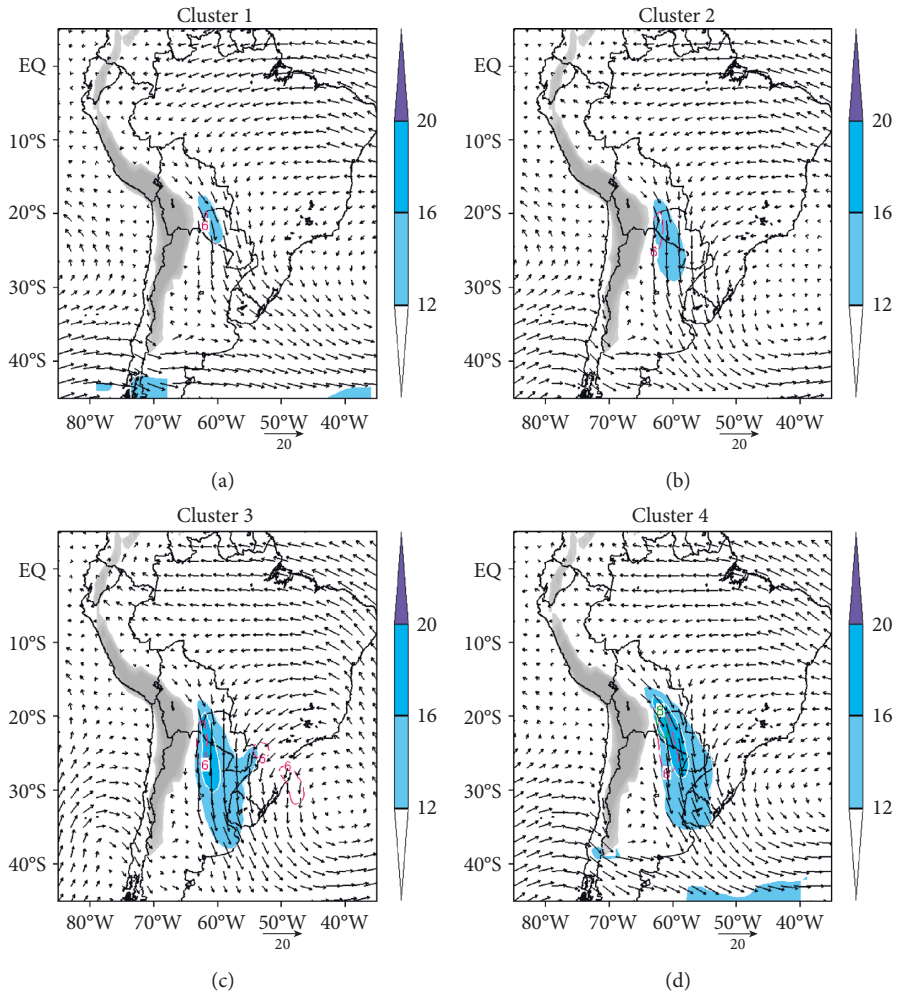

Figure 9: Composite wind fields for each cluster: wind (*vector*); wind speed (*shaded*) at 850 hPa, and wind shear between 850 hPa and 700 hPa (*red contours*). *Shaded*: wind intensity stronger than 12 m·s^{-1}. *Red contours*: wind shear greater than 6 m·s^{-1}. Terrain elevations higher than 1500 m are shown.

Table 2: Mean AOD500nm and AE_440–870nm for each trajectory cluster.

Cluster #	All		BB		No BB	
	AOD500nm	AE_440–870	AOD500nm	AE_440–870	AOD500nm	AE_440–870
1	0.354	1.514	0.560	1.576	0.179	1.460
2	0.338	1.570	0.514	1.621	0.182	1.526
3	0.390	1.638	0.654	1.755	0.179	1.544
4	0.543	1.660	0.721	1.697	0.187	1.586

The first two columns present the results for the whole data set whereas the second and third pairs of columns correspond to biomass-burning season (BB) and no-burning period (no BB), respectively.

along with those on the selected days when CJ1 and biomass burning occurred simultaneously.

The results presented here are consistent with published research. The selected days exhibit statistically significant increase in aerosol optical depth and Ångström exponent. The peak in volume size distribution in the fine mode moves towards larger concentrations and shifts slightly towards bigger diameters. Overall aerosol behaviour on days when AOD is greater than 0.15 is similar to that reported in other urban sites with urban/industrial and biomass-burning pollution. The analysis of the biomass-burning days clearly shows that higher values of AOD and Ångström exponent, together with negative Ångström exponent differences and dominant fine fraction, are linked to biomass-burning particle dispersion by long-range transport.

A trajectory cluster analysis was made to identify the CJ1 modes that most contribute to the long-range transport of biomass-burning aerosols. The cluster whose trajectories

include air masses travelling along the jet core is the one displaying the greatest influence on aerosol spectral properties.

The results contribute to advance in the characterization of aerosol particles in Buenos Aires city and to the assessment of short and long-range impacts of air pollution. The role of regional flow as an agent connecting remote sources with the city was analysed, and the fingerprint of biomass-burning was shown. This study used common tools and methods to make comparisons possible of the results obtained herein with the published literature.

Data Availability

The GDAS meteorological data are available at https://www.ncdc.noaa.gov/data-access/model-data/model-datasets/global-data-assimilation-system-gdas from NOAA's National Climatic Data Center. AERONET information is available at https://aeronet.gsfc.nasa.gov/. The HYSPLIT model and the meteorological files to drive the simulations can be found at https://www.ready.noaa.gov/HYSPLIT.php.

Conflicts of Interest

The author declares that there are no conflicts of interest regarding the publication of this paper.

Acknowledgments

This research was partially funded by the Project UBACyT 20020130100771 in Argentina. Thanks are due to B. Holben and AERONET PIs for collecting the aerosol observations worldwide. NOAA is acknowledged for the meteorological data and the HYSPLIT model.

References

[1] INDEC, *Censo Nacional de Población, Hogares y Viviendas 2010, Censo del Bicentenario: Resultados Definitivos*, Instituto Nacional de Estadística y Censos, Buenos Aires, Argentina, in Spanish, 1st edition, 2012.

[2] S. T. Martin, M. O. Andreae, P. Artaxo et al., "Sources and properties of Amazonian aerosol particles," *Reviews of Geophysics*, vol. 48, no. 2, p. RG2002, 2010.

[3] K. M. Longo, S. R. Freitas, M. O. Andreae, A. Setzer, E. Prins, and P. Artaxo, "The coupled aerosol and tracer transport model to the Brazilian developments on the regional atmospheric modeling system (CATT-BRAMS)-part 2: model sensitivity to the biomass burning inventories," *Atmospheric Chemistry and Physics*, vol. 10, no. 13, pp. 5785–5795, 2010.

[4] M. Andreae, "Biomass burning: its history, use and distribution and its impact on environmental quality and global climate," in *Global Biomass Burning: Atmospheric, Climatic and Biospheric Implications*, J. S. Levine, Ed., pp. 3–21, MIT Press, Cambridge, UK, 1991.

[5] UNEP-CCAC, "Integrated assessment of short-lived climate pollutants for Latin America and the Caribbean: improving air quality while mitigating climate change," in *Summary for Decision Makers*, G. Raga and P. Artaxo, Eds., p. 198, United Nations Environment Programme and Climate and Clean Air Coalition United Nations Environment Programme, Nairobi, Kenya, 2018.

[6] C. Vera, J. Baez, M. Douglas et al., "The South American low-level jet experiment," *Bulletin of the American Meteorological Society*, vol. 87, no. 1, pp. 63–78, 2006.

[7] J. A. Marengo, B. Liebmann, A. M. Grimm et al., "Recent developments on the South American monsoon system," *International Journal of Climatology*, vol. 32, no. 1, pp. 1–21, 2012.

[8] P. Salio, M. Nicolini, and E. J. Zipser, "Mesoscale convective systems over southeastern South America and their relationship with the south American low-level jet," *Monthly Weather Review*, vol. 135, no. 4, pp. 1290–1309, 2007.

[9] J. Paegle, "A comparative review of South American low level jets," *Meteorologica*, vol. 23, pp. 73–81, 1998.

[10] A. G. Ulke, K. M. Longo, and S. R. Freitas, "Biomass burning in South America: transport patterns and impacts," in *Biomass—Detection, Production and Usage*, D. Matovic, Ed., InTech, Rijeka, Croatia, 2011.

[11] S. R. Freitas, K. M. Longo, M. A. F. Silva Dias et al., "Monitoring the transport of biomass burning emissions in South America," *Environmental Fluid Mechanics*, vol. 5, no. 1-2, pp. 135–167, 2005.

[12] S. R. Freitas, K. M. Longo, M. A. F. Silva Dias et al., "The coupled aerosol and tracer transport model to the Brazilian developments on the regional atmospheric modeling system (CATT-BRAMS)-part 1: model description and evaluation," *Atmospheric Chemistry and Physics*, vol. 9, no. 8, pp. 2843–2861, 2009.

[13] M. E. Castañeda and A. G. Ulke, "Analysis of atmospheric conditions associated to CHACO events of the Low Level Jet East of the Andes and their implications for regional transport," *International Journal of Climatology*, vol. 35, no. 14, pp. 4126–4138, 2015.

[14] A. G. Ulke, "Aerosol characterization in Buenos Aires and relationships with transport patterns in South America," *Ciencia e Natura*, pp. 193–196, 2009.

[15] A. G. Ulke, S. R. Freitas, and K. M. Longo, "Aerosol load and characteristics in Buenos Aires: relationships with dispersion mechanisms and sources in South America," in *Air Pollution Modeling and its Application XXI*, D. G. Steyn and S. T. Castelli, Eds., pp. 251–255, Springer, Dordrecht, The Netherlands, 2012.

[16] H. D. Kambezidis and D. G. Kaskaoutis, "Aerosol climatology over four AERONET sites: an overview," *Atmospheric Environment*, vol. 42, pp. 1892–1906, 2008.

[17] T. F. Eck, B. N. Holben, I. Slutsker, and A. Setzer, "Measurements of irradiance attenuation and estimation of aerosol single scattering albedo for biomass burning aerosols in Amazonia," *Journal of Geophysical Research: Atmospheres*, vol. 103, no. D24, pp. 31865–31878, 1998.

[18] J. S. Reid, P. V. Hobbs, R. J. Ferek et al., "Physical, chemical, and optical properties of regional hazes dominated by smoke in Brazil," *Journal of Geophysical Research: Atmospheres*, vol. 103, no. D24, pp. 32059–32080, 1998.

[19] T. F. Eck, B. N. Holben, J. S. Reid et al., "High aerosol optical depth biomass burning events: a comparison of optical properties for different source regions," *Geophysical Research Letters*, vol. 30, no. 20, p. 2035, 2003.

[20] Y. J. Kaufman, "Aerosol optical thickness and atmospheric path radiance," *Journal of Geophysical Research: Atmospheres*, vol. 98, no. D2, pp. 2677–2692, 1993.

[21] T. F. Eck, B. N. Holben, J. S. Reid et al., "Wavelength dependence of the optical depth of biomass burning, urban, and desert dust aerosols," *Journal of Geophysical Research: Atmospheres*, vol. 104, no. D24, pp. 31333–31349, 1999.

[22] N. T. O'Neill, O. Dubovik, and T. F. Eck, "A modified Ångström coefficient for the characterization of sub-micron aerosols," *Applied Optics*, vol. 40, no. 15, pp. 2368–2375, 2001.

[23] G. L. Schuster, O. Dubovik, and B. N. Holben, "Angstrom exponent and bimodal aerosol size distributions," *Journal of Geophysical Research*, vol. 111, no. D7, Article ID D07207, 2006.

[24] G. P. Gobbi, Y. J. Kaufman, I. Koren, and T. F. Eck, "Classification of aerosol properties derived from AERONET direct sun data," *Atmospheric Chemistry and Physics*, vol. 7, no. 2, pp. 453–458, 2007.

[25] B. N. Holben, T. F. Eck, I. Slutsker et al., "AERONET—a federated instrument Network and data archive for aerosol characterization," *Remote Sensing of Environment*, vol. 66, no. 1–16, 1998.

[26] A. Smirnov, B. N. Holben, T. F. Eck, O. Dubovik, and I. Slutsker, "Cloud-Screening and quality control algorithms for the AERONET database," *Remote Sensing of Environment*, vol. 73, no. 3, pp. 337–349, 2000.

[27] O. Dubovik, A. Smirnov, B. N. Holben et al., "Accuracy assessments of aerosol optical properties retrieved from Aerosol Robotic Network (AERONET) Sun and sky radiance measurements," *Journal of Geophysical Research: Atmospheres*, vol. 105, no. D8, pp. 9791–9806, 2000.

[28] N. T. O'Neill, T. F. Eck, A. Smirnov et al., "Spectral discrimination of coarse and fine mode optical depth," *Journal of Geophysical Research*, vol. 108, no. D17, pp. 4559–4573, 2003.

[29] D. M. Giles, A. Sinyuk, M. G. Sorokin et al., "Advancements in the Aerosol Robotic Network (AERONET) Version 3 database—automated near-real-time quality control algorithm with improved cloud screening for Sun photometer aerosol optical depth (AOD) measurements," *Atmospheric Measurement Techniques*, vol. 12, no. 1, pp. 169–209, 2019.

[30] R. R. Draxler and G. D. Hess, "An overview of the HYSPLIT-4 modelling system for trajectories, dispersion, and deposition," *Australian Meteorological Magazine*, vol. 47, pp. 295–308, 1998.

[31] A. F. Stein, R. R. Draxler, G. D. Rolph, B. J. B. Stunder, M. D. Cohen, and F. Ngan, "NOAA's HYSPLIT atmospheric transport and dispersion modeling system," *Bulletin of the American Meteorological Society*, vol. 96, no. 12, pp. 2059–2077, 2015.

[32] S. Basart, C. Pérez, E. Cuevas, J. M. Baldasano, and G. P. Gobbi, "Aerosol characterization in Northern Africa, Northeastern Atlantic, Mediterranean Basin and Middle East from direct-sun AERONET observations," *Atmospheric Chemistry and Physics*, vol. 9, no. 21, pp. 8265–8282, 2009.

[33] D. G. Kaskaoutis, S. Kumar Kharol, P. R. Sinha et al., "Extremely large anthropogenic-aerosol contribution to total aerosol load over the Bay of Bengal during winter season," *Atmospheric Chemistry and Physics*, vol. 11, no. 14, pp. 7097–7117, 2011.

[34] R. R. Draxler, B. Stunder, G. Rolph et al., *HYSPLIT4 Users Guide*, NOAA Air Resources Laboratory, Silver Spring, MD, USA, 2015, http://ready.arl.noaa.gov/HYSPLIT.php.

[35] K. Longo, S. Freitas, A. G. Ulke et al., "Transport of biomass burning products in southeastern South America and its relationship with the south American low level jet East of the Andes," in *Proceedings of 8 ICSHMO*, pp. 121–129, Foz do Iguaçu, Brazil, April 2006.

[36] C. Toledano, M. Wiegner, S. Groß et al., "Optical properties of aerosol mixtures derived from sun-sky radiometry during SAMUM-2," *Tellus B: Chemical and Physical Meteorology*, vol. 63, no. 4, pp. 635–648, 2011.

[37] D. Pérez-Ramírez, M. Andrade-Flores, T. F. Eck et al., "Multi year aerosol characterization in the tropical Andes and in adjacent Amazonia using AERONET measurements," *Atmospheric Environment*, vol. 166, pp. 412–432, 2017.

[38] O. Dubovik, B. Holben, T. F. Eck et al., "Variability of absorption and optical properties of key aerosol types observed in worldwide locations," *Journal of the Atmospheric Sciences*, vol. 59, no. 3, pp. 590–608, 2002.

[39] J. S. Reid and P. V. Hobbs, "Physical and optical properties of young smoke from individual biomass fires in Brazil," *Journal of Geophysical Research: Atmospheres*, vol. 103, no. D24, pp. 32013–32030, 1998.

[40] P. R. Sinha, D. G. Kaskaoutis, R. K. Manchanda, and S. Sreenivasan, "Characteristics of aerosols over Hyderabad in southern Peninsular India: synergy in the classification techniques," *Annales Geophysicae*, vol. 30, no. 9, pp. 1393–1410, 2012.

[41] X. Yu, R. Lü, C. Liu et al., "Seasonal variation of columnar aerosol optical properties and radiative forcing over Beijing, China," *Atmospheric Environment*, vol. 166, pp. 340–350, 2017.

[42] J. Zhu, X. Xia, H. Che, J. Wang, J. Zhang, and Y. Duan, "Study of aerosol optical properties at Kunming in southwest China and long-range transport of biomass burning aerosols from North Burma," *Atmospheric Research*, vol. 169, pp. 237–247, 2016.

[43] D. G. Kaskaoutis, P. R. Sinha, V. Vinoj et al., "Aerosol properties and radiative forcing over Kanpur during severe aerosol loading conditions," *Atmospheric Environment*, vol. 79, pp. 7–19, 2013.

[44] D. G. Kaskaoutis, R. Gautam, R. P. Singh et al., "Influence of anomalous dry conditions on aerosols over India: transport, distribution and properties," *Journal of Geophysical Research: Atmospheres*, vol. 117, no. D9, 2012.

[45] C. Guirado, E. Cuevas, V. E. Cachorro et al., "Aerosol characterization at the Saharan AERONET site Tamanrasset," *Atmospheric Chemistry and Physics*, vol. 14, no. 21, pp. 11753–11773, 2014.

[46] A. K. Mishra and T. Shibata, "Synergistic analyses of optical and microphysical properties of agricultural crop residue burning aerosols over the Indo-Gangetic Basin (IGB)," *Atmospheric Environment*, vol. 57, pp. 205–218, 2012.

[47] A. Valenzuela, F. J. Olmo, H. Lyamani et al., "Aerosol transport over the western Mediterranean basin: evidence of the contribution of fine particles to desert dust plumes over Alborán Island," *Journal of Geophysical Research: Atmospheres*, vol. 119, no. 24, pp. 14028–14044, 2014.

[48] T. F. Eck, B. N. Holben, D. E. Ward et al., "Characterization of the optical properties of biomass burning aerosols in Zambia during the 1997 ZIBBEE field campaign," *Journal of Geophysical Research: Atmospheres*, vol. 106, no. D4, pp. 3425–3448, 2001.

[49] B. N. Holben, D. Tanré, A. Smirnov et al., "An emerging ground-based aerosol climatology: aerosol optical depth from AERONET," *Journal of Geophysical Research: Atmospheres*, vol. 106, no. D11, pp. 12067–12097, 2001.